



Influence of pH on the release of an active principle from 3D printed carrageenan-k combined with alginate or xanthan gum

Dhanalakshmi Vadivel^{a,b,*}, Nicolò Zitarosa^a, Daniele Dondi^{a,b}

^a Department of Chemistry, University of Pavia, Viale Taramelli 12, 27100, Pavia, Italy

^b INFN, Sezione di Pavia, Via Agostino Bassi 6, 27100, Pavia, Italy

ARTICLE INFO

Keywords:

3D bioprinting
pH
Drug release
Hydrogel
Polymer
Dye

ABSTRACT

The use of 3D printing began to diffuse in the pharmaceutical field in recent times, since 2015, with the approval of the first 3D printed drug from the FDA. The most used materials in association with this technique in this specific scope are hydrogels, already used widely in tissue engineering to produce scaffolds used in the realization of synthetic tissues. The aim of this project was to study the influence of different pH conditions on the release of a therapeutic molecule from a Carrageenan-k combined with alginate or xanthan gum hydrogel with a high level of biocompatibility and enough mechanical resistance to be used as printing material for a 3D bioprinter. The addition of biologically active supplements without affecting the model of the 3D printing structure of the biocompatible polymers was achieved by adopting the extrusion at moderately low temperatures. This study aimed to produce the necessary percentage of hydrogels which is responsible for the release of active drugs which respect to the pH of the system. In this case, the chosen curcumin drug which exhibits active release in the pH of the small intestine is a pH value of 6.

1. Introduction

Hydrogels are polymers that can produce 3D structures in the hydrophilic water-rich environment straight forwarding by forming cross-linked chains which involve thermally induced entanglement of polymer chains [1], molecular self-assembly [2], ionic gelations [3], electrostatic interaction [4] and chemical cross-linking [5]. Physical and chemical properties of the hydrogels can be tuned in a smart way rendering them stimuli-responsive exploiting their active recognition moieties [6]. The versatility of hydrogels brings them to different applications in diverse fields like sensors [7], actuators [8], soft electronics [9] and the biomedical field [10]. Hydrogels can be modified through click chemistry [11,12], doping with nanomaterials and a combination of hydrogels to achieve the right physicochemical properties [13–15].

Natural polymers, which are derived from plants, animals and algae are commonly polysaccharides and proteins and tend to form thermally reversible hydrogels. With respect to the temperature change, the physical entanglement process of the polymer chain arises during the gelation process [16]. This change is typically caused by an alteration in their solubility.

Since the invention of 3D printing (Fig. 1) in the twentieth century [17], the technologies on which the creation of physical objects designed using 3D modeling software is based mainly into broad categories: printing by extrusion [18] and stereolithography [19], inkjet printing, fused deposition method, laser-assisted sintering [20].

* Corresponding author. Department of Chemistry, University of Pavia, Viale Taramelli 12, 27100 Pavia, Italy.
E-mail address: dhanalakshmi.vadivel@unipv.it (D. Vadivel).

The first category can exploit multiple extrusion mechanisms (giving the possibility to build multi-material objects) but all are united by the outflow of the material, which is deposited on a plate that generally remains fixed, while the extruder moves along the X, Y and Z axes. Stereolithography instead uses photosensitive resins, placed inside a tank or boat, where the printing surface is immersed; a light source (an LED, LASER or LCD projector) of the preferred wavelength to hit the resin according to the instructions given to the printer causes it to polymerize into a solid object on the bed.

Bioprinting is a forthcoming branch that mainly refers to the broader category of 3D printing by extrusion, born from the desire to apply this extremely precise and versatile technology to the medical-pharmaceutical field [21]. The need for compounds that could mimic the mechanical characteristics of the plastic materials used in normal 3D printing processes and at the same time were biocompatible to the point of being able to act as a culture medium for cell growth [22], led to the birth of bio-inks, a term with which hydrogels or mixtures of them are indicated, with rheological characteristics that can be applied to 3D printing and biocompatibility high enough to be approved for medical use [23]. The refinement of bioprinting techniques, which led to the production of scaffolds that can be used for cell growth [22], continues its evolution, so much so that it has played an important role in tissue engineering for the production of complex tissues and organs. The most common technique in the field of bioprinting is the hot extrusion of a bio-ink on a flat surface [24]. In the pharmaceutical field, 3D printing is gaining more and more importance in the design of customized dosage that guarantees high control over the drug release [25] allowing for an improvement in therapeutic efficacy.

The introduction of bioprinting in the pharmaceutical field is destined to have a disruptive impact, thanks to this technology it is possible to produce medicines in small batches, controlling for each of their dosage, shape, size and release kinetics [25,26] fundamental characteristics for a personalized approach towards which modern medicine is evolving. In 2015, the Food and Drug Administration (FDA) approved the first 3D-printed drug, and research has since begun to develop innovative formulations using this approach. Obviously, there are still many obstacles related to its use on a large scale; high costs based on the development of new formulations or the redesign of existing formulations and the maintenance of the equipment that guarantees the pharmaco-technical properties of the final product. Despite the very high versatility of this technique, there are no standards but the compatibility between an active ingredient and the excipients within a drug must be established experimentally, case by case [25].

Bio-responsive hydrogels [27] are widely used related to the release of insulin in the needed higher blood glucose level in the treatment of insulin-dependent diabetes. In this case, the basic polymeric carrier is immobilized with glucose oxidase enzyme which is responsible to convert glucose into gluconic acid. This formulation tends to increase the acidity which protonated the basic groups of the polymer thus enhancing the releasing profile of insulin. On the other hand, while insulin is released, the sugar level drops which stops the unnecessary release of further negative feedback.

The term drug delivery includes all the production techniques, formulations and technologies commonly used in the pharmaceutical industry to improve the transport of an active ingredient to its target, with the aim of enhancing the therapeutic action of the drug. It is a process of extreme importance aimed at regulating the pharmacokinetics, therefore the processes of absorption, distribution, metabolism and elimination (ADME) [28] of a substance, guaranteeing advantages both at a therapeutic level and in patient compliance. In targeted drug delivery, developing the systems which can reach the needed site before the drug start to be released is a major task that agrees with the improved drug release strategy that can cause maximum drug absorption at the diseased site.

Curcumin or diferuloylmethane is the main curcuminoid (a subfamily of polyphenols) contained within the rhizome of *Curcuma Longa*, a herbaceous perennial plant, very common in the Asian continent [29]. It is a molecule known since ancient times as it is contained in turmeric. Today it is recognized and used around the world in many different forms due to its beneficial effects. To date, curcumin has been shown to possess antioxidant properties, it is, in fact, capable of promoting the activity within the serum of antioxidant molecules such as superoxide dismutase (SOD) and catalase, but also has anti-inflammatory properties being able to block the activation of NF- κ B, a transcription factor which in turn is an activator of tumour necrosis factor α (TNF- α) one of the most common inflammatory mediators [30] involved in the development of many chronic diseases including Alzheimer's and some neoplastic

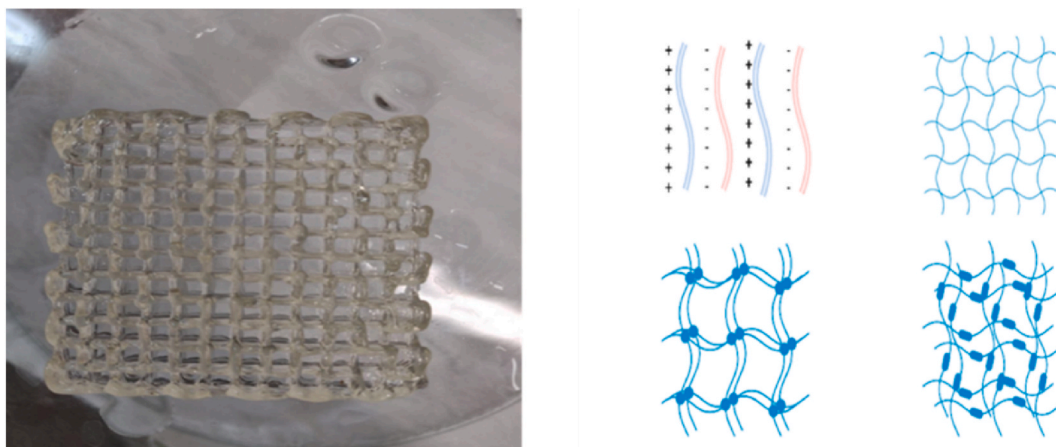


Fig. 1. Sodium alginate lattice made by 3D printing (left) and interactions between the chains of a hydrogel (right).

diseases.

Despite the numerous positive effects, the biggest problem with curcumin is its poor intestinal absorption and rapid metabolism [30] which results in extremely reduced bioavailability. Curcumin appears as unstable at basic pH by degrading to *trans*-6-(4'-hydroxy-3'-methoxyphenyl)-2,4-dioxo-5-hexanal, ferulic acid, feruloyl methane and vanillin within 30 min, while the degradation it is slower in acidic conditions, with less than 20% of curcumin decomposed in 1 h [28]. Many excipients have been tested to overcome this limitation, such as the simultaneous administration of the active ingredient to piperine, an alkaloid present in black pepper, capable of reducing its metabolism, but also the use of nanoparticles and liposomes (being a very lipophilic molecule) able to incorporate the curcumin molecule and allow its transport into the bloodstream at the level of the cells, where, once internalized, the vesicles release the active ingredient.

The choice of polymers for the current work is all natural origin and easy to find, already widely used as excipients in the food and pharmaceutical industries, with very low toxicity, water-soluble and capable of forming gels with different viscosities. The printability of the hydrogel was assessed by viscosimetric analysis then the qualified mixture of hydrogels was engaged for the drug release in a trial-and-error method. Selected compounds include carrageenan-k, alginate (Fig. 2) and xanthan gum. Carrageenan is a natural polymer, extracted from red algae, with low toxicity and high biocompatibility due to its properties of extracellular matrix mimetic. The most interesting propriety of this polymer is its thermo-sensibility which grants the possibility to extrude the material in liquid form at high temperatures and obtain a rapid solidification while cooling down. In this project it was decided to use the molten deposition method, exploiting the gelation characteristics of the hydrogels, in relation to the temperature difference between the extruder and the surface, in a very similar way to how the same method is applied in plastic materials. The main problem with using pure carrageenan solidified layers is that they do not stick together causing a structural defect in the structure. To fix this problem, two-hybrid formulations were investigated by mixing the thermosensitive properties of carrageenan with the other two polymers. Dyes were used in the basic trial experiments and the results were transferred in controlling the release of a drug, Curcumin, under precise pH conditions.

2. Materials and methods

2.1. Materials

Carrageenan-k and xanthan gum bought from Saporepuro. Sodium alginate bought from CARLO ERBA. They were chosen from commercially food-grade available samples and characterized (see supplementary information). Other reagents Methylene blue, Rhodamine B and curcumin were bought from Sigma-Aldrich.

2.2. Emulsion preparation

The emulsion was prepared by using distilled water and Triton X-100 stirred for 30 min at a ratio. To this solution curcumin (final curcumin concentration in the gel is $1 \times 10^{-5} \text{ mol dm}^{-3}$) is added and stirred at 27°C with homogenized for 30 min. Other emulsions with methylene blue and Rhodamine B were prepared using distilled water stirred for 30 min at a ratio of (final concentration of methylene blue and Rhodamine in the gel is $1 \times 10^{-5} \text{ mol dm}^{-3}$). All these three mixtures are kept separate and then prepared with different compositions of chosen polymers carrageenan-k, alginate and xanthan gum. By trial-and-error method using viscosity measurement, we figured out the right percentage of polymers for the fluid intended for 3D printing.

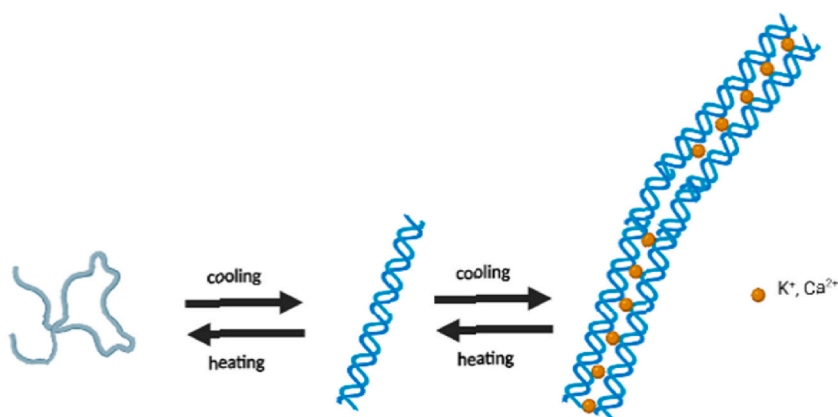


Fig. 2. Change in the lattice structure of alginate according to the change in temperature.

2.3. Rheological characterization

2.3.1. Analytical methods

To identify the polymer capable of forming the gel with the most suitable characteristics to be used as a bio-ink, the materials were characterized from the physical point of view through a rotational viscometer [31] and from the chemical-physical point of view through FT-infrared spectrophotometry (FT-IR) (S7–S9) and thermogravimetric analysis (TGA) (S1–S6) in a two different atmospheric condition (N₂ and air). Because, in presence of air all the carbon materials are burned, show that the inorganic traces become thermally stable oxides. This study allows us to understand the amount of carbon material existence in the sample. In presence of N₂ atmosphere, most of the organic molecules can burn and converted into solid carbon (like pyrolytic carbon).

2.3.2. Viscosity analysis

Viscosity is the most important parameter to define the behaviour of a fluid intended for 3D printing. The characteristics to look for in a material that can be considered suitable for this type of production process include thermo-sensitivity, shear-thinning and high recovery capacity. This means that the ideal hydrogel must have a high viscosity at room temperature, at the same time this viscosity is inversely proportional to the shear stress and to the temperature in order to guarantee fluid extrusion through the nozzle of the printer (a 1 mm diameter needle in this experiment) and which is able to maintain the shape of a semi-solid filament when the shear stress is released, strong enough to withstand the weight of the overlying structure without collapsing. The pressure to the syringe and nozzle is approximately 0.5 bar.

A standard protocol for the preparation of the hydrogels was defined, which were then subjected to a viscosity analysis in order to obtain preliminary information on their possible behaviour during the extrusion process. The analyses were carried out using a rotational viscometer: an instrument capable of measuring viscosity (expressed in centipoise) on the basis of the shear stress of a cylindrical bar called “spindle” with respect to its rotation speed within the solution. This has allowed us to divide the solutions into two categories, namely those in which the shear stress is proportional to the rotation speed and those in which this proportionality does not exist, i.e., to separate the Newtonian fluids from the non-Newtonian ones.

The behaviour of a Newtonian fluid can be explained in equation (1)

$$\tau = \mu \frac{\Delta\psi}{\Delta y} \quad (1)$$

Where τ is the shear stress exerted by the fluid and expressed in Pascal, μ is the dynamic viscosity of the fluid, also expressed in Pascal and $\Delta\psi/\Delta y$ is the velocity gradient perpendicular to the direction of the deformation, it follows that the graph of τ as a function of $\Delta\psi/\Delta y$ will be a straight line, therefore it is a fluid with constant viscosity. In a non-Newtonian fluid, the viscosity varies according to the shear stress that is applied and therefore it is not constant, there are many different subtypes, but the hydrogels mostly have a pseudo-plastic behaviour [32] in which the viscosity decreases as the deformation rate increases and thixotropic, in which viscosity decreases over time. So, the viscosity we observed in these tests is non-Newtonian fluid behaviour for both mixtures.

For each material, solutions were prepared to be subjected to viscosimetric analysis at different concentrations by dissolving the compound in 400 ml of distilled water and heated to 70 °C, using a mechanical stirrer. Each solution was mixed for about 1 h until a homogeneous gel was formed. The viscosity study for each hydrogel was carried out based on the two most relevant parameters to obtain an optimal extrusion in terms of 3D printing; the viscosity variation in relation to the variation of the temperature and the shear stress was analyzed.

Each compound was analyzed at 3 different temperatures with an interval of 10 °C between one and the other: 65 °C, 55 °C and 45 °C. Due to the difficulty of thermosetting the solution during the analysis, it is present a standard deviation of ± 2 °C in the reported data, which however did not prove significant as regards the accuracy of the results obtained on the viscosity of the solutions. For each different temperature, the viscosity was then tested at 3 different rotation speeds of the spindle: 30, 50 and 60 RPM (revolutions per minute) to determine its behaviour with the variation of the shear stress. For each compound, an ideal minimum and a maximum concentration were defined, of which the viscosity was analyzed and reported in the form of a graph expressed in centipoises. Based on the data collected, the following parameters were defined as standards for the analysis of the dye release kinetics: room temperature, absence of agitation and integration time of 10.0 s. The spindle number R7 is used for dyes and drug release experiments. We use up to R5 when we make trial experiments for a highly viscous mixture of samples.

2.4. Material printing

A 3Drag chocolate printer (Futura Elettronica, Italy) was used to realize the samples in this phase. This 3D printer model is characterized by a fixed extruder that consent to charge high volumes of gel on the Z-axis without reducing the printing precision because printed object movements are made from the mobile bed along the X and Y-axes.

Normally printers used for bioprinting mount pressure extrusion systems with syringes having a capacity of a few ml, so as not to hinder the movements of the extruder along the cartesian axes, but the need to print relatively large samples, in the order of several cm³, required the use of a printer capable of working with large syringes, up to 100 ml, without affecting the quality of the print. For this reason, it was decided to use a printer that mounted a fixed extruder on the Z axis and a movable plane along the X and Y axes like the 3Drag model in its “chocolate printer” version (S10 and S11). It is a printer compatible with open-source software designed by the Futura Elettronica/ElettronicaIn teams, which allows the printing of objects with a maximum size of 20 × 20 × 20 cm. Unlike the

standard configuration, designed for filament fusion printing with plastic materials, mainly ABS (acrylonitrile butadiene styrene) and PLA (polylactic acid), this version is equipped with an extruder equipped with a heating jacket in which it is possible to insert a syringe through which the material is extruded under the pressure of a piston. It is a model designed for use in the food sector that allows the use of melted chocolate as a material for making objects, whose solidity is controlled by the temperature of the extruder and the surface. This type of system was chosen because of the common characteristics of viscosity, but above all thermo-sensitivity that chocolate and hydrogels have in common. The printer is also equipped with a cooling system based on Peltier cells to increase the solidification speed of the object. However, due to the low printing speed used in this work, the system was not used.

The printing parameters have been identified by trial and error regulating the printing temperature and the bed movement speed. Both the hybrid gels showed good printability during the printing process and different objects in terms of shape complexity and dimension were analyzed. The first step was finding the right material based on some essential characteristics described in the literature before biocompatibility, low toxicity, natural origin, edibility, low environmental impact, low costs and ability to form high viscosity gels in water.

The biggest difficulty that we find ourselves facing in this area is identifying the correct bio-ink, despite the wide range of proposals on the market: each material has unique characteristics that determine a wide variability in the results [33].

2.5. Buffer solution preparation

For pH 3 and 6 buffer solutions were first prepared in two 0,05 M citric acid solutions by dissolving 5 g of citric acid in 500 ml of water, then a concentrated NaOH solution (5 M) has been added ml by ml to the acidic solution while constantly measuring the pH until the target values. For the 7 and 8 solutions were first prepared two 0,05 M acidic solutions, mixing 2.5 g of phosphoric acid with 500 ml of water, then the solutions have been brought to pH by adding a NaOH solution in the same way.

2.6. Curcumin release analysis

The preparation of a hydrogel containing curcumin required the addition of a further compound, Triton X-100, a non-ionic surfactant, that is, an amphiphilic compound with a polar head and an apolar tail, capable of lowering the surface tension, to increase the wet-ability of the surfaces, this to allow the dissolution of curcumin, otherwise insoluble in water. 2.5 ml of Triton X-100 which appears as a very viscous compound was added to 200 ml of distilled water and slowly mixed with a mechanical stirrer to prevent the formation of bubbles, once a homogeneous solution was formed, 0.015 g of curcumin was added and the solution was brought to 70 °C. Subsequently, carrageenan- κ and then the second biopolymer were added, xanthan gum in one case and alginate in the other. The printing of the samples and the spectrophotometric analysis was carried out following the same model applied to the analysis of dyes, taking a sample of buffer solution every 30 min, for a total of 6 measurements in 180 min. To better understand drug selectivity, we applied two different dyes, methylene blue and rhodamine B, to a mixture of two types of hydrogels.

3. Results and discussion

3.1. Rheological properties

3.1.1. Viscosity measurement

The viscosity of carrageenan- κ is measured at a different temperature with alginate and xanthan gum to carry out printing stability.

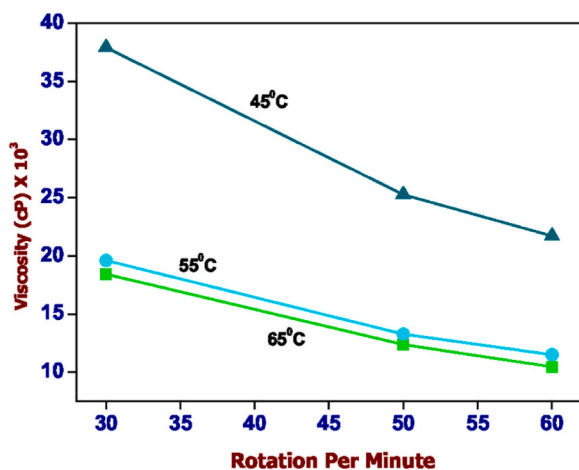


Fig. 3. Viscosity values of a hydrogel containing 2% carrageenan- κ and 2% xanthan gum in the temperature range of 65 °C (green), 55 °C (blue) and 45 °C (cyan). (For interpretation of the references to colour in this figure legend, the reader is referred to the Web version of this article.)

To forecast their hydrogel performance during the printing process the hydrogels were subjected to viscometric analysis at different temperatures and shear rates, to find the variation of viscosity in the complement of temperature, concentration, and shear stress. The analysis was carried out using a rotational viscometer to study the viscosity of gels at three different temperatures: 65 °C, 55 °C and 45 °C. The tests show how carrageenan- κ thermosensitive properties are maintained in the two-hybrid formulations, showing a drastic increase of thickness under 55 °C. For both formulations, at every temperature 3 different spindle rotation speeds are studied 30, 50 and 60 RPM, showing a non-Newtonian, pseudo-plastic operation of the viscosity of the gel decreasing as shear stress increases [32].

Fig. 3 shows the change in viscosity measurements with respect to rotation per minute at 45 °C, 55 °C and 65 °C of the hydrogel sample containing carrageenan- κ (2%) with xanthan gum (2%). The high-temperature 65 °C of measure has a lower viscosity than the sample heating up to 55 °C. The sample heating up to 45 °C shows higher viscosity in less rotation per minute then it becomes moderate with respect to the rotation per minute. In Fig. 4, the same trend of the experiment got followed in the hydrogel sample mixture of carrageenan (4%) with alginate (1%), heating up to 65 °C, 55 °C and 45 °C. The temperature chosen for the printing accessibility with respect to the hydrogel formation, in both cases the temperature chosen for the print test is 45 °C.

3.2. Hydrogel print test

Despite the excellent properties demonstrated and the degree of precision achieved, the integrity and solidity of the objects in pure carrageenan are not sufficient, the layers tend to separate at the slightest mechanical action or to dissolve quickly if immersed in water or subjected to temperatures above 45 °C, for this reason, we arrived at the addition of xanthan gum and alginate, which proved to be able to overcome the limits of carrageenan. In various layers increasing the integrity of the printed object, in the case of alginate, the crosslinking was performed with a 20% solution of calcium nitrate. Both carrageenan- κ -based hybrid gels were initially tested to produce a 5 cm-sided scaffold, divided into 3 mm-sided cells (Fig. 5), to evaluate the maintenance of accuracy with the new material. Above all sufficient integrity to manipulate the object and remove it from the plane.

The positive outcome of this test is possible to switch to objects with a more relevant height and a square-based pyramid with both sides of the base and a height of 3 cm was created with both hydrogels which are shown in Fig. 5. The step forward compared to the use of carrageenan alone is not appropriate because of texture to the touch and, above all, able to withstand the mechanical stress of medium entity but more precise and bilateral.

For the dye release test, the model of a cube (Fig. 6) with a side of 2 cm and a filling of 15% was used, using the same concentrations of compounds for the two hydrogels (alginate with calcium nitrate and xanthan gum) and the same printing parameters in terms of speed and temperature. It was decided to move from the pyramid to the cube for a practical concern, this shape has in fact guaranteed a more homogeneous release of the dye from all the faces and edges of the solid, regardless of its position during the floating inside the buffer solution.

3.3. Spectrophotometric analysis

All the analyses on the dye release were carried out at room temperature in the absence of agitation. For each test, 4 beakers of 250 ml were prepared each containing 50 ml of a different pH buffered solution in which a cube of hydrogel containing the dye is dropped. The tests lasted a total of 180 min. In each case, the absorbance of the buffer solutions was measured every 30 min by taking a sample of 3 ml of solution each time. The samples of the buffer solutions at pH 7.00 and 8.00, in the tests on the hydrogel based on carrageenan and alginate, required a further filtration step due to the reaction of calcium ions with the phosphates present in the buffer, causing the formation of insoluble calcium phosphate, which made the solution to be analyzed cloudy, altering the absorbance values found.

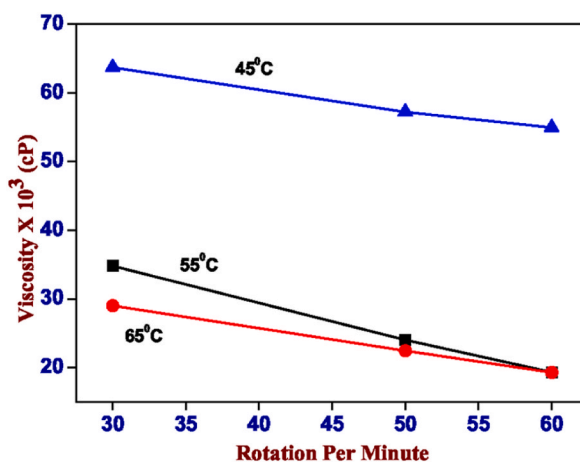


Fig. 4. Viscosity values of a hydrogel containing 4% carrageenan- κ and 1% sodium alginate in the temperature range of 65 °C (red), 55 °C (black) and 45 °C (blue). (For interpretation of the references to colour in this figure legend, the reader is referred to the Web version of this article.)

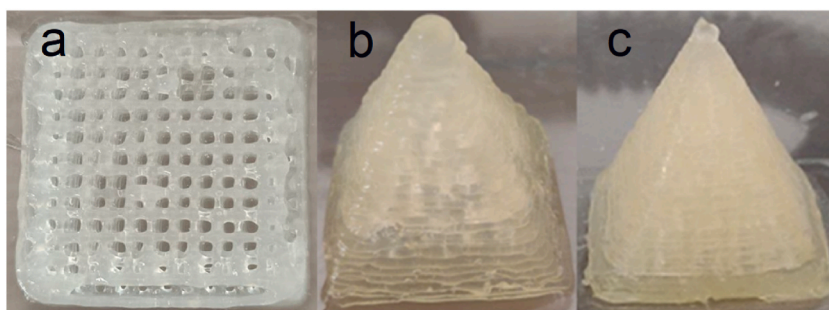


Fig. 5. A) Carrageenan-xanthan gum scaffold, b) carrageenan-alginate (left) and c) carrageenan-xanthan gum (right) pyramids.

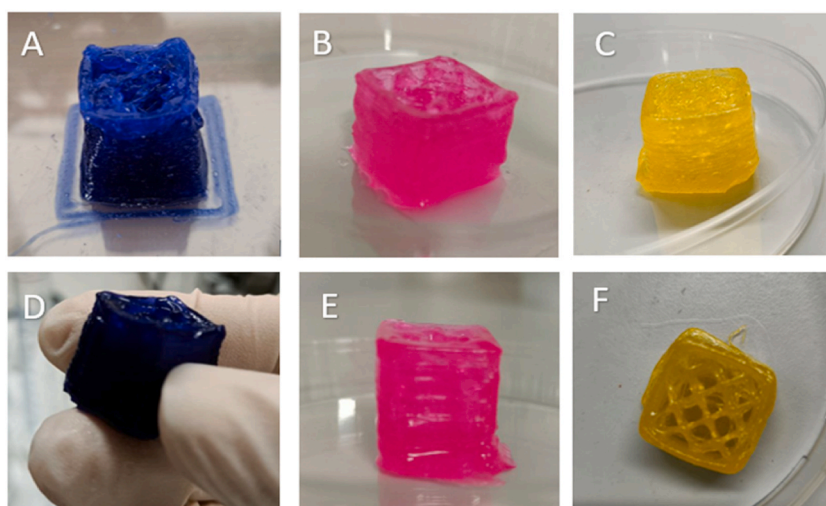


Fig. 6. Cubes with 2 cm side composed of 1% alginate and 4% carrageenan- κ (A, B, C) and 2% xanthan gum and 2% carrageenan- κ (D, E, F) made by 3D printing, containing methylene blue (A, D) Rose Bengal (B, E) and curcumin (C, F). (For interpretation of the references to colour in this figure legend, the reader is referred to the Web version of this article.)

Through the spectrophotometric analysis, the absorbance curves were obtained as a function of the wavelength for each sample; the values of the absorption peaks were at this point extrapolated and subjected to a further processing step. It was necessary to apply a correction with respect to the baseline, which is the reference point with respect to which the variance of the variables was calculated. For each curve obtained by spectrophotometric analysis, the X and Y coordinates of points A, B and C were extrapolated and the following formula was applied as explained in equation (2)

$$B_y - (B_x - A_x) \cdot \left[\frac{(C_y - A_y)}{(C_x - A_x)} \right] + A_y \quad (2)$$

The formula applied represents the first-order polynomial and allows a type of linear correction with respect to the baseline. It was possible to apply a linear and non-exponential correction since the variation in values is not high; consequently, the error generated is negligible compared to the data obtained. The values of the maximum absorbance peak obtained through the application of the correction were then tabulated and reported in the form of a graph, classifying them according to the dye used.

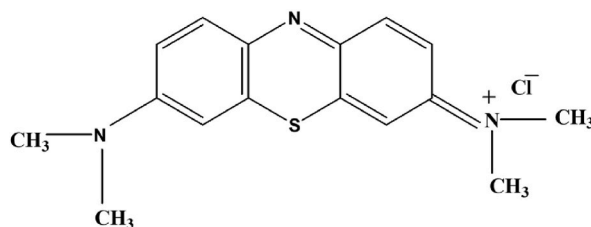


Fig. 7. Methylene blue chemical structure.

3.4. Controlled release: probe tests

Two sets of samples were prepared for each hydrogel, the first one containing methylene blue and the second one containing Rose Bengal. Each set has been immersed in four buffer solutions with different pHs (3, 6, 7 and 8) to mimic the different conditions of the gastrointestinal tract. The release of dye in the different conditions was measured by spectrophotometric analysis to study the variation of absorbance in the function of time.

3.4.1. Methylene blue

The absorbance values obtained from the spectrophotometric analysis of the release of methylene blue from the two gel mixtures (Figs. 9 and 10), show the test with the least significant results with respect to the pH change, showing the same behaviour in all the pH. It is difficult to extrapolate information from the values obtained, if not a clearly lower release under basic conditions as it is also visible for samples soaked for 180 min (Fig. 8). This is because the dye has cationic characteristics (Fig. 7) while both (alginate with calcium nitrate and xanthan gum) hydrogels are anionic, for these reasons the interaction between methylene blue and the polymeric chains of the hydrogels causes an altered release. This is probably due to the interactions between the MB + cation with the COO-groups present on the alginate and xanthan gum [34].

In the xanthan gum, the fat globules have a size of around 60–80 μm which is dispersed in a xanthan gum water-based phase mixture. This xanthan gum water mixture is highly specific in the stomach pH level when it's acidic specifically. Because xanthan gum in an acidic pH benefits the physical contact of the fat globules that weaken the matrix. Therefore, the viscoelastic behaviour of xanthan gum decreases by the less electrostatic repulsion at acidic pH, favouring the curcumin-like drug release [35]. But in the case of methylene blue, it already reacts with xanthan gum fat globules that hinder the participation of contact between them. This may cause a stable structure that never allows the dye to be released from the matrix.

3.4.2. Rose Bengal

Rose Bengal in water tends to acquire a negative charge (Fig. 11) generating repulsive forces with the carboxylic groups of the polymers that make up the hydrogels. This type of interaction generates much more interesting results that show the release of dye is significantly greater for both hydrogels (alginate with calcium nitrate and xanthan gum) which are shown in Figs. 13 and 14 (see Fig. 12).

It can be noted that the pH range at which we have the greatest release is between 6.00 and 7.00. The absorbance reaches values of 0.122 in the case of the mixture of carrageenan with alginate (Fig. 13) and a greater extent of 0.756 was observed in that of carrageenan with xanthan gum (Fig. 14) at pH 6.00. While, for both gels, it is extremely low at basic pH (>7) and almost zero in conditions of greater acidity ($\text{pH} < 6$). This means that the two hybrid hydrogels release most of their content under similar pH conditions (pH 6–7) to those of the small intestine, i.e., the gastrointestinal tract area where the absorption surface is greater for drugs that come under this caliber shows better bioavailability for any drug inserted into the gel mixture.

3.5. Controlled release: the active principle

The tests were repeated by substituting the dyes with curcumin (Fig. 15) as an active principle by keeping the hydrogels preparations discussed above. The preparation of a hydrogel containing curcumin required the addition of a further compound, Triton X-100. Subsequently, the printing of the samples and the spectrophotometric analysis was carried out following the same model applied to the analysis of dyes, taking a sample of buffer solution every 30 min, for a total of 6 measurements in 180 min.

For each hydrogel were printed a set of samples containing curcumin and the spectrophotometric analysis was repeated multiple times under the same conditions, confirming the data obtained with the curcumin to be sure and comparing with Rose Bengal. In fact, also in this curcumin case, the highest release is at pH 6 visible in Fig. 16. For this reason, it is safe to hypothesize the excipient-like behaviour of the two hydrogels tested as carriers of active principles through the gastrointestinal tract to the intestine to grant the release which shown in Figs. 17 and 18.



Fig. 8. Carrageenan and Xanthan Gum cubes were immersed in buffer solutions at pH 6.00, 7.00 and 8.00.

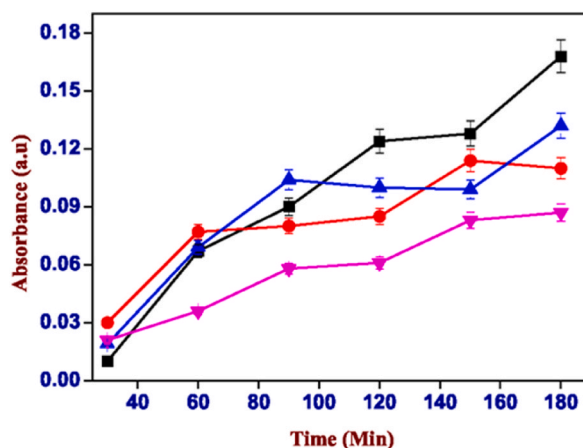


Fig. 9. Absorbance values of the solution of carrageenan-k (4%) and alginate (1%) containing methylene blue, black: pH 3.00, blue: pH 7.00, red: pH 6.00 and pink: pH 8.00. (For interpretation of the references to colour in this figure legend, the reader is referred to the Web version of this article.)

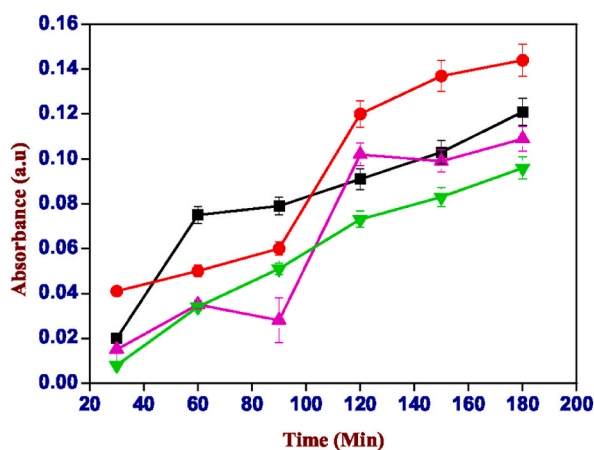


Fig. 10. Absorbance values of the solution of carrageenan-k (2%) and xanthan gum (2%) containing methylene blue, red: pH 6.00, black: pH 3.00, pink: pH 7.00 and green: pH 8.00. (For interpretation of the references to colour in this figure legend, the reader is referred to the Web version of this article.)

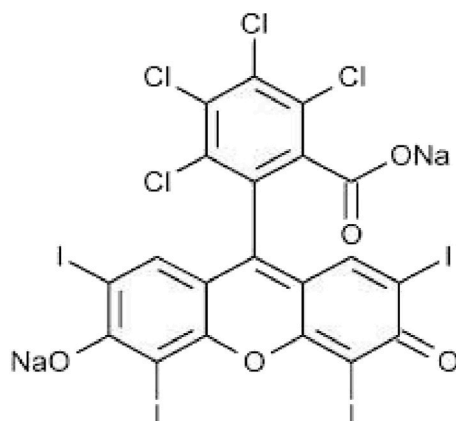


Fig. 11. Rose Bengal chemical structure.



Fig. 12. Carrageenan and Xanthan Gum cubes were immersed in buffer solutions at pH 6.00, 7.00 and 8.00.

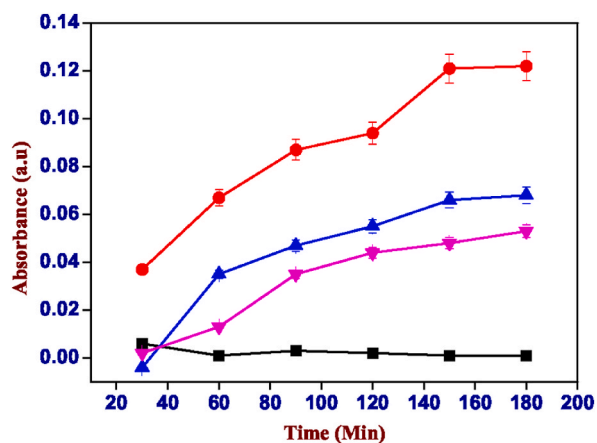


Fig. 13. Absorbance values of the solution of carrageenan-k (4%) and alginate (1%) containing Rose Bengal, red: pH 6.00, blue: pH 7.00, pink: pH 8.00 and cyan: pH 3.00. (For interpretation of the references to colour in this figure legend, the reader is referred to the Web version of this article.)

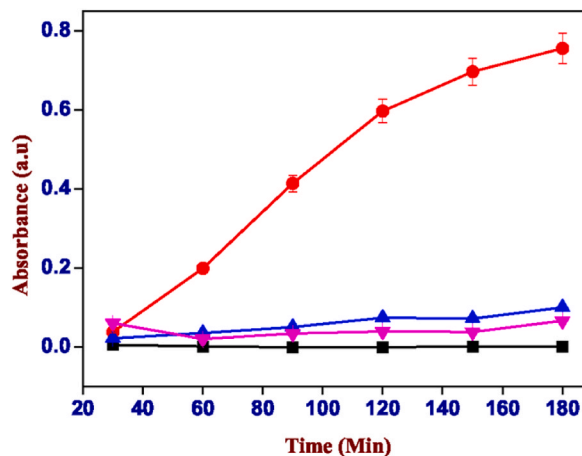


Fig. 14. Absorbance values of the solution of carrageenan-k (2%) and xanthan gum (2%) containing Rose Bengal, red: pH 6.00, blue: pH 7.00, pink: pH 8.00 and black: pH 3.00. (For interpretation of the references to colour in this figure legend, the reader is referred to the Web version of this article.)

4. Conclusion

By exploiting the intrinsic characteristics of carrageenan, combined with those of alginate and xanthan gum, two hydrogels with sufficient mechanical stability to be manipulated were realized to print three-dimensional constructs with high precision while maintaining good biocompatibility. Depending on the different pH conditions, it is possible to obtain the controlled release of an active

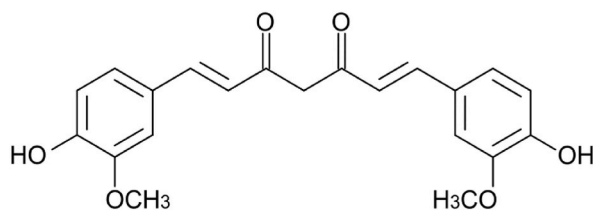


Fig. 15. Structural formula of the Curcumin.

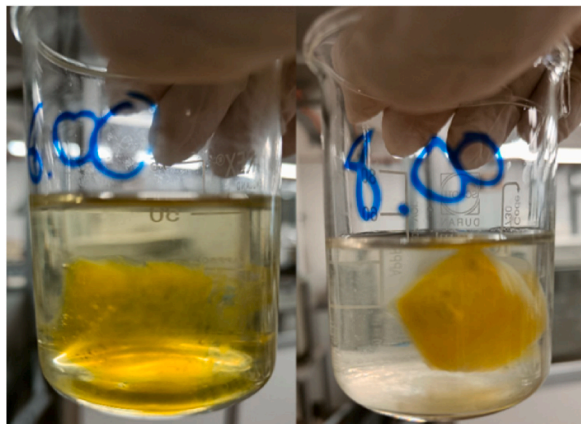


Fig. 16. Difference in the release of curcumin by two identical samples of carrageenan- κ and xanthan gum at pH 6.00 (left) and at pH 8.00 (right).

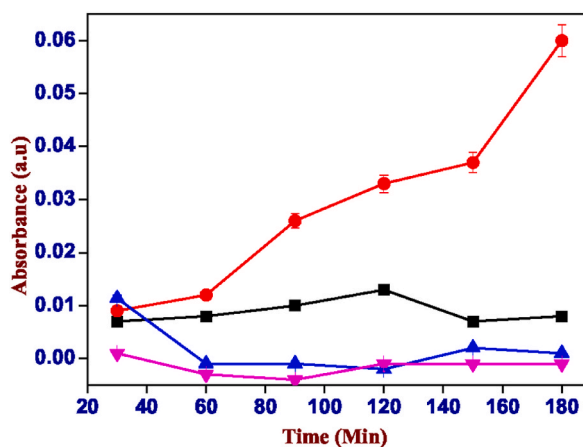


Fig. 17. Absorbance values of the solution of carrageenan-k (4%) and alginate (1%) containing curcumin, red: pH 6.00, black: pH 7.00, blue: pH 8.00 and pink: pH 3.00. (For interpretation of the references to colour in this figure legend, the reader is referred to the Web version of this article.)

ingredient which is maximized in acidic conditions with pH values around 6. These same acidity values can be found within the small intestine [36]. With the developed method it is therefore possible to obtain a biocompatible construct, controllable in terms of shape, size, content and speed of release in the gastrointestinal tract.

Author contribution statement

Dhanalakshmi Vadivel: Analyzed and interpreted the data; Wrote the paper; Conceived and designed the experiments.

Nicolò Zitarosa: Performed the experiments.

Daniele Dondi: Contributed reagents, materials, analysis tools or data; Conceived and designed the experiments.

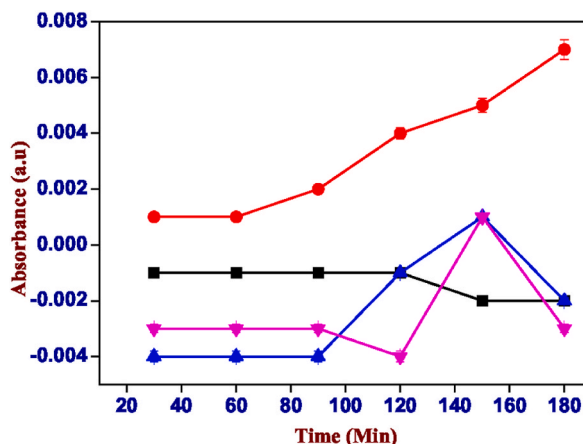


Fig. 18. Absorbance values of the solution of carrageenan-k (2%) and xanthan gum (2%) containing curcumin, red: pH 6.00, black: pH 7.00, blue: pH 8.00 and pink: pH 3.00. (For interpretation of the references to colour in this figure legend, the reader is referred to the Web version of this article.)

Data availability statement

Data will be made available on request.

Declaration of competing interest

The authors declare that they have no known competing financial interests or personal relationships that could have appeared to influence the work reported in this paper.

Acknowledgment

D.D. and D.V. acknowledge support from the Ministry of University and Research (MUR) and the University of Pavia through the program “Dipartimenti di Eccellenza 2023–2027.”

Appendix A. Supplementary data

Supplementary data to this article can be found online at <https://doi.org/10.1016/j.heliyon.2023.e16850>.

References

- [1] Z. Tang, D. Liu, X. Lyu, Y. Liu, Y. Liu, W. Yang, Z. Shen, X. Fan, *J. Mater. Chem. C* 10 (30) (2022), 10926, <https://doi.org/10.1039/D2TC01721K>.
- [2] Y.S. Liu, R.D. Chakravarthy, A.A. Saddik, M. Mohammed, H.C. Lin, *RSC Adv.* 12 (22) (2022) 14315–14320, <https://doi.org/10.1039/D2RA01944B>.
- [3] A. Mirek, H. Belaid, F. Barranger, M. Grzeczko, Y. Bouden, V. Cavaillès, D. Lewińska, M. Bechelany, *J. Mater. Chem. B* 10 (43) (2022) 8862–8874, <https://doi.org/10.1039/D2TB01268E>.
- [4] S. Ye, W. Ma, W. Shao, O. Ejeromedoghene, G. Fu, M. Kang, *Polymer* 243 (2022), 124642, <https://doi.org/10.1016/j.polymer.2022.124642>.
- [5] P. Rahmani, A. Shojaei, *Polymer* 254 (2022), 125037, <https://doi.org/10.1016/j.polymer.2022.125037>.
- [6] I. Amarsy, S. Papot, G. Gasser, *Angew. Chem. Int. Ed.* 61 (40) (2022), <https://doi.org/10.1002/anie.202205900>.
- [7] T. Zhang, L. Meng, Y. Hu, Z. Ouyang, W. Li, B. Xie, F. Zhu, J. Wan, Q. Wu, *RSC Adv.* 12 (36) (2022) 23637–23643, <https://doi.org/10.1039/D2RA03822F>.
- [8] Y. Zhao, J. Cui, X. Qiu, Y. Yan, Z. Zhang, K. Fang, Y. Yang, X. Zhang, J. Huang, *Adv. Colloid Interface Sci.* 308 (2022), 102749, <https://doi.org/10.1016/j.cis.2022.102749>.
- [9] D. Gao, J. Lv, P.S. Lee, *Adv. Mater.* 34 (25) (2022), 2105020, <https://doi.org/10.1002/adma.202105020>.
- [10] Y. Li, H.Y. Yang, D.S. Lee, *Biomacromolecules* 23 (3) (2022) 609–618, <https://doi.org/10.1021/acs.biomac.1c01552>.
- [11] Z. Tang, D. Liu, X. Lyu, Y. Liu, Y. Liu, W. Yang, Z. Shen, X. Fan, *J. Mater. Chem. C* 10 (30) (2022), 10926, <https://doi.org/10.1039/D2TC01721K>.
- [12] T.T. Vu, M. Gulfam, S.-H. Jo, S.-H. Park, K.T. Lim, *Carbohydr. Polym.* 278 (2022), 118964, <https://doi.org/10.1016/j.carbpol.2021.118964>.
- [13] S. Kim, Y. Choi, W. Lee, K. Kim, *Tissue Eng. Regen. Med.* 19 (2) (2022) 309–319, <https://doi.org/10.1007/s13770-021-00413-5>.
- [14] J. Dadashi, M.A. Ghasemzadeh, M. Salavati-Niasari, *RSC Adv.* 12 (36) (2022) 23481–23502, <https://doi.org/10.1039/D2RA03418B>.
- [15] M. Piazzoni, A. Negri, E. Brambilla, L. Giussani, S. Pitton, S. Caccia, S. Epis, C. Bandi, S. Locarno, C. Lenardi, *Soft Matter* 18 (34) (2022) 6443–6452, <https://doi.org/10.1039/D2SM00889K>.
- [16] L. Cao, Z. Zhao, J. Li, Y. Yi, Y. Wei, *Biomacromolecules* 23 (3) (2022) 1278–1290, <https://doi.org/10.1021/acs.biomac.1c01506>.
- [17] P. Ghosal, B. Gupta, R.S. Ambekar, M.M. Rahman, P.M. Ajayan, N. Aich, A.K. Gupta, C.S. Tiwary, *Adv. Sustain. Syst.* 6 (3) (2022), 2100282, <https://doi.org/10.1002/adsu.202100282>.
- [18] J. Zhang, Y. Li, Y. Cai, I. Ahmad, A. Zhang, Y. Ding, Y. Qiu, G. Zhang, W. Tang, F. Lyu, *Carbohydr. Polym.* 294 (2022), 119763, <https://doi.org/10.1016/j.carbpol.2022.119763>.

- [19] K. Ogishi, T. Osaki, Y. Morimoto, S. Takeuchi, *Lab Chip* 22 (5) (2022) 890–898, <https://doi.org/10.1039/D1LC01077H>.
- [20] Y. He, F. Yang, H. Zhao, Q. Gao, B. Xia, J. Fu, *Sci. Rep.* 6 (1) (2016), 29977, <https://doi.org/10.1038/srep29977>.
- [21] C.J. Picco, J. Domínguez-Robles, E. Utomo, A.J. Paredes, F. Volpe-Zanutto, D. Malinova, R.F. Donnelly, E. Larrañeta, *Drug Deliv.* 29 (1) (2022) 1038–1048, <https://doi.org/10.1080/10717544.2022.2057620>.
- [22] G. Luo, Y. Ma, X. Cui, L. Jiang, M. Wu, Y. Hu, Y. Luo, H. Pan, C. Ruan, *RSC Adv.* 7 (20) (2017) 11880–11889, <https://doi.org/10.1039/C6RA27669E>.
- [23] S.E. Evans, T. Harrington, M.C. Rodríguez Rivero, E. Rognin, T. Tuladhar, R. Daly, *Int. J. Pharm.* 599 (2021), 120443, <https://doi.org/10.1016/j.ijpharm.2021.120443>.
- [24] F. Cleymand, A. Poerio, A. Mamanov, K. Elkhoury, L. Ikhelf, J.P. Jehl, C.J.F. Kahn, M. Poçot, E. Arab-Tehrany, J.F. Mano, *Bioprinting* 21 (2021), e00122, <https://doi.org/10.1016/j.bprint.2020.e00122>.
- [25] M. Pandey, H. Choudhury, J.L.C. Fern, A.T.K. Kee, J. Kou, J.L.J. Jing, H.C. Her, H.S. Yong, H.C. Ming, S.K. Bhattamisra, B. Gorain, *Drug Deliv. Transl. Res.* 10 (4) (2020) 986–1001, <https://doi.org/10.1007/s13346-020-00737-0>.
- [26] S.J. Trenfield, A. Awad, A. Goyanes, S. Gaisford, A.W. Basit, *Trends Pharmacol. Sci.* 39 (5) (2018) 440–451, <https://doi.org/10.1016/j.tips.2018.02.006>.
- [27] G. Fundueanu, M. Constantin, M. Turtoi, S.-M. Bucatariu, B. Cosman, M. Anghelache, G. Voicu, M. Calin, *Pharmaceutics* 14 (4) (2022) 865, <https://doi.org/10.3390/pharmaceutics14040865>.
- [28] A.J. Lucas, J.L. Sproston, P. Barton, R.J. Riley, *Expet Opin. Drug Discov.* 14 (12) (2019) 1313–1327, <https://doi.org/10.1080/17460441.2019.1660642>.
- [29] R.A. Sharma, A.J. Gescher, W.P. Steward, *Eur. J. Cancer* 41 (13) (2005) 1955–1968, <https://doi.org/10.1016/j.ejca.2005.05.009>.
- [30] S. Hewlings, D. Kalman, *Foods* 6 (10) (2017) 92, <https://doi.org/10.3390/foods6100092>.
- [31] M.H. Kim, J.N. Lee, J. Lee, H. Lee, W.H. Park, *ACS Biomater. Sci. Eng.* 6 (5) (2020) 3103–3113, <https://doi.org/10.1021/acsbmaterials.0c00411>.
- [32] L.A. Shah, T.U. Rehman, M. Khan, *Polym. Bull.* 77 (8) (2020) 3921–3935, <https://doi.org/10.1007/s00289-019-02951-4>.
- [33] A. Bhattacharyya, G. Janarthanan, H.N. Tran, H.J. Ham, J. Yoon, I. Noh, *Chem. Eng. J.* 415 (2021), 128971, <https://doi.org/10.1016/j.cej.2021.128971>.
- [34] C.B. Godiya, Y. Xiao, X. Lu, *Int. J. Biol. Macromol.* 144 (2020) 671–681, <https://doi.org/10.1016/j.ijbiomac.2019.12.139>.
- [35] M. Espert, A. Salvador, T. Sanz, *Food Hydrocolloids* 95 (2019) 454–461, <https://doi.org/10.1016/j.foodhyd.2019.05.004>.
- [36] J. Fallingborg, *Dan. Med. Bull.* 46 (3) (1999 Jun) 183–196. PMID: 10421978.